SUPPLEMENTARY INFORMATION

Ethanol-Induced Suppression of GIRK-Dependent Signaling in the Basal Amygdala

Marron Fernandez de Velasco *et al.*

SUPPLEMENTAL METHODS AND MATERIALS

Intracranial viral manipulations

The AAV8-CaMKIIα-mCherry virus was produced by the University of Minnesota Viral Vector and Cloning Core (VVCC; Minneapolis, MN), using pAAV-CaMKIIα-hChR2(C128S/D156A)-mCherry (Addgene plasmid #35502, a gift from Dr. Karl Deisseroth) as the backbone (1). The AAV8-CaMKIIα-Cre(mCherry) virus was obtained from the University of North Carolina Vector Core (Chapel Hill, NC). Titers were between 0.43-1.34 x 10^{14} genocopies/mL. Mice (7-8 weeks old) were placed in a stereotaxic device (David Kopf Instruments; Tujunga, CA) under isoflurane anesthesia. Microinjectors were made by affixing a 33-gauge stainless steel hypodermic tube within a shorter 26-gauge stainless steel hypodermic tube. The microinjectors were attached to polyethylene-20 tubing affixed to 10 μl Hamilton syringes, and were lowered through burr holes in the skull to the BA (from bregma: −1.65 mm A/P, ±3.25 mm M/L, −4.7 mm D/V): 400 nl of viral solution per side was injected over 4 min. The syringe was left in place for 10 min following infusion to reduce solution backflow along the infusion track.

Electrophysiological and behavioral experiments were performed 4-5 wk after surgery to allow for full recovery and viral expression. The scope and accuracy of viral targeting was assessed using fluorescence microscopy following the completion of behavioral studies, by an investigator blind to subject treatment. Images were acquired from coronal slices (250 μm) of the BLA and overlaid using ImageJ and evaluated using the Allen Mouse Brain Atlas as a reference (2). Targeting was deemed acceptable if: a) it was bilateral, with comparable intensity of viral-driven fluorescence on both sides of the brain; b) the center of viral infection was within the boundary of the BA, and; c) >60% of labeling was confined to the BA. If targeting was deemed unacceptable, associated data from this subject were not included in the final analysis.

Fluorescence multiplex in situ hybridization. Adult mice (8 wk) were anesthetized with halothane and decapitated. Brains were rapidly extracted and flash frozen in isopentane at -50°C for 20 s. Frozen brains were wrapped in aluminum foil and stored at -80°C until further use. Brains were equilibrated in the cryostat at -20°C for 2 h before BLA coronal sections (16 μM) were collected and mounted onto Superfrost Plus slides (Fisher). After sectioning, slides were stored at -80°C until further processing. For processing, slides were transferred to slide racks and the sections were fixed in 4% paraformaldehyde for 1 h at 4°C. Slides were rinsed twice with PBS, followed by dehydration in 50%, 70%, and 100% ethanol, and storage in fresh 100% ethanol at -20°C overnight. The next day, slides were dried for 5 min at room temperature

(RT) and a hydrophobic pen (ImmEdge Hydrophobic Barrier Pen, Vector Laboratories) was used to create a barrier around the slices to contain labeling reagents. Sections were incubated in hydrogen peroxide (10 min at RT), followed by incubation in a solution containing protease IV (30 min at RT). Sections were incubated in 1x target probes for specific RNAs: CaMKIIα-C1 and CaMKIIα-C2 probes (NM_009792.3; target nt region, 896-1986), GIRK1-C1 (NM_008426.2; target nt region, 658-1679), GIRK2-C3 (NM_001025584.2; target nt region, 282-1456), and GIRK3-C2 (NM_008429.2; target nt region, 84-1276) for 2 h at 40°C using a HybEZ hybridization oven (Advanced Cell Diagnostics). Following the hybridization step, sections were incubated with preamplifier and amplifier probes followed by fluorescently labeled probes with specific color-channel combinations: green, red, near infrared (Opal 520, Opal 620, Opal 690, respectively; Akoya Biosciences). Sections were incubated with DAPI for 20s to stain nuclei (blue), and then mounted with glass coverslips using ProLong Gold Antifade (ThermoFisher Scientific). Slides were dried for 30 min at RT before being stored at -20°C.

Behavioral test battery #1

Handling-induced convulsions (Day 1). Mice were picked up by the tail and monitored for convulsions after being twirled by the tail along a 360° arc. Convulsion signs were rated by an experimenter blind to the treatment condition, using a severity scale from 0 to 5, as described (3). A score of '0' was given when there were no movements after the twirl; scores from 1 to 5 were assigned according to the severity of observed hind leg, body jerks, or body twists observed.

Light-dark box (Day 2). The light-dark test was conducted using two-compartment chambers (16.76 x 12.7 x 12.7 cm) housed within sound-attenuating cubicles and software (MED-PC IV 4.2) from Med Associates, Inc. Chamber compartments were equally sized with the light side containing white floors, walls, and overhead illumination (single 2.8-W light bulb) and the dark side containing black floors and walls only with no illumination. Animals were placed in the dark side of the light/dark box, facing the entrance to the light chamber and their activity was monitored via infrared beam breaks throughout a 15 min test period. The percentage of time spent in the light side of the chamber was extracted for analysis.

Marble burying test (Day 4). Mice were removed from their home cages and single housed in clean polycarbonate mouse cages (18 x 28 x 13 cm) containing 4-5 cm of aspen wood chip

bedding; mice were allowed to habituate to the novel substrate for 5 mins. The mice were then removed from the cage and placed in another holding cage while 20 dark blue marbles (1.15-cm diameter) were arranged in a 4 x 5 array in the testing cage. Mice were returned to the corner of the testing cages containing aspen bedding and marbles for a period of 30 min. The number of marbles that were buried (more than 75% of the marble was covered by bedding) were counted at the end of the test. Mice were then single housed with *ad libitum* access to food and water after the marble burying test.

Bottle brush test (Days 6 and 7). Irritability-like behavior was tested on Day 6 and 7 using the bottle brush test, as described (4). Aggressive and defensive responses to "attacks" by a moving brush were measured as irritability-like behavior. The test was conducted during the dark phase under red lighting. Single-housed animals were attacked 10 times with 10 s intertrial intervals in their home cage with the lid and food tray removed. During each trail, the mouse started at the opposite end of the cage and was attacked by a brush rotating towards it from the front of the cages, eventually touching its whiskers. The brush was then rotated back to the starting position where it remained rotating for approximately 2 s, and then was allowed to hang vertically for approximately the same amount of time. Aggressive (smelling/exploring the brush, following the brush) and defensive (escaping, rearing, digging/burying, jumping) responses to these repeated attacks were recorded. A sum of aggressive and defensive responses across all 10 trials was measured and averaged across the 2 test days to calculate an irritability-like behavior score.

Behavioral test battery #2

Elevated plus maze (Day 1). Performance in elevated plus maze (EPM) and fear conditioning tests was examined in a separate cohort of C57BL/6J mice subjected to the CIE/4 treatment protocol, in battery fashion. EPM was evaluated first, 2 d after the final ethanol or air-treatment session (Day 2). EPM testing conditions were as described previously (5).

Fear conditioning (Day 3). To permit detection of either an increase or decrease in conditioned fear, we used an established delay fear conditioning protocol involving 1 CS/US pairing (6). On the first day of fear conditioning (Day 3), mice were trained using a single 30-s auditory cue (CS; white noise/65 dB) that co-terminated with a 2-s foot-shock (US; 0.50 mA). Time spent freezing

following re-exposure to the context without CS presentation (Day 4), and CS presentation in a novel context (Day 5), were used to assess contextual and cue fear memory, respectively.

Immunoelectron microscopy. Immunohistochemical reactions for electron microscopy were carried out using the pre-embedding immunogold method described previously (7). Briefly, free-floating sections were incubated in 10% (v/v) NGS diluted in TBS. Sections were then incubated in anti-GIRK2 or anti-$GABA_{B1}$ antibodies [3-5 μg/mL diluted in TBS containing 1% (v/v) NGS], followed by incubation in goat anti-rabbit or anti-mouse IgG coupled to 1.4 nm gold (Nanoprobes Inc., Stony Brook, NY, USA), respectively. Sections were postfixed in 1% (v/v) glutaraldehyde and washed in double-distilled water, followed by silver enhancement of the gold particles with an HQ Silver kit (Nanoprobes Inc.). Sections were then treated with osmium tetraoxide (1% in 0.1 M phosphate buffer), block-stained with uranyl acetate, dehydrated in graded series of ethanol and flat-embedded on glass slides in Durcupan (Fluka) resin. Regions of interest were cut at 70-90 nm on an ultramicrotome (Reichert Ultracut E, Leica, Austria) and collected on single slot pioloform-coated copper grids. Staining was performed on drops of 1% aqueous uranyl acetate followed by Reynolds's lead citrate. Ultrastructural analyses were performed in a JEOL JEM-1400Flash electron microscope.

Quantification of GIRK2 channel and $GABA_{B1}$ receptor immunoreactivities. To establish the relative abundance of GIRK2 and $GABA_{B1}$ in control conditions and after ethanol treatment, immunoreactivity in different compartments of principal neurons in the BA and LA, we used 60-μm-thick coronal slices processed for pre-embedding immunogold immunohistochemistry, as described (7). Briefly, for each of four animals per experimental group, samples of tissue were obtained for the preparation of embedding blocks. To minimise false negatives, electron microscopic serial ultrathin sections were cut close to the surface of each block, as immunoreactivity decreased with depth. We estimated the quality of immunolabelling by always selecting areas with optimal gold labelling at approximately the same distance from the cutting surface. Randomly selected areas were then captured with a high sensitivity sCMOS camera at magnifications of 30,000X. Quantification of immunolabelling was performed in 2 different ways:

1. *Immunoparticles for GIRK2 and $GABA_{B1}$ subunits.* We counted immunoparticles identified in each reference area and present in different subcellular compartments: plasma membrane and intracellular sites.

2. *Density of GIRK2 and $GABA_{B1}$ proteins along the plasma membrane.* To establish the density of GIRK2 and $GABA_{B1}$ along the surface of principal neurons in the BA and LA, we performed quantification of immunolabelling in 60-µm-thick coronal slices processed for pre-embedding immunogold. Immunoparticles identified in the plasma membrane of principal neurons were counted and the perimeter of the subcellular compartment containing the immunoparticles was measured (ImageJ). The data, linear density of GIRK2 and $GABA_{B1}$ in each neuronal compartment in control conditions and after ethanol treatment, were expressed as the number of immunoparticles/µm.

Antibodies and chemicals. The following primary antibodies were used: rabbit anti-GIRK2 (Rb-Af290; aa. 390–421 of mouse GIRK2A-1; RRID: AB_2571712; Frontier Institute Co. Japan) and mouse anti-$GABA_{B1}$ (clone N93A/49, Neuromab, CA, USA). The characteristics and specificity of the anti-GIRK2 antibody have been described elsewhere (8). The characteristics and specificity of the antibody targeting $GABA_{B1}$ has been described by the manufacturer. The secondary antibodies used were goat anti-rabbit IgG coupled to 1.4 nm gold and goat anti-mouse IgG coupled to 1.4 nm gold (1:100; Nanoprobes Inc., Stony Brook, NY, USA).

SUPPLEMENTAL FIGURES

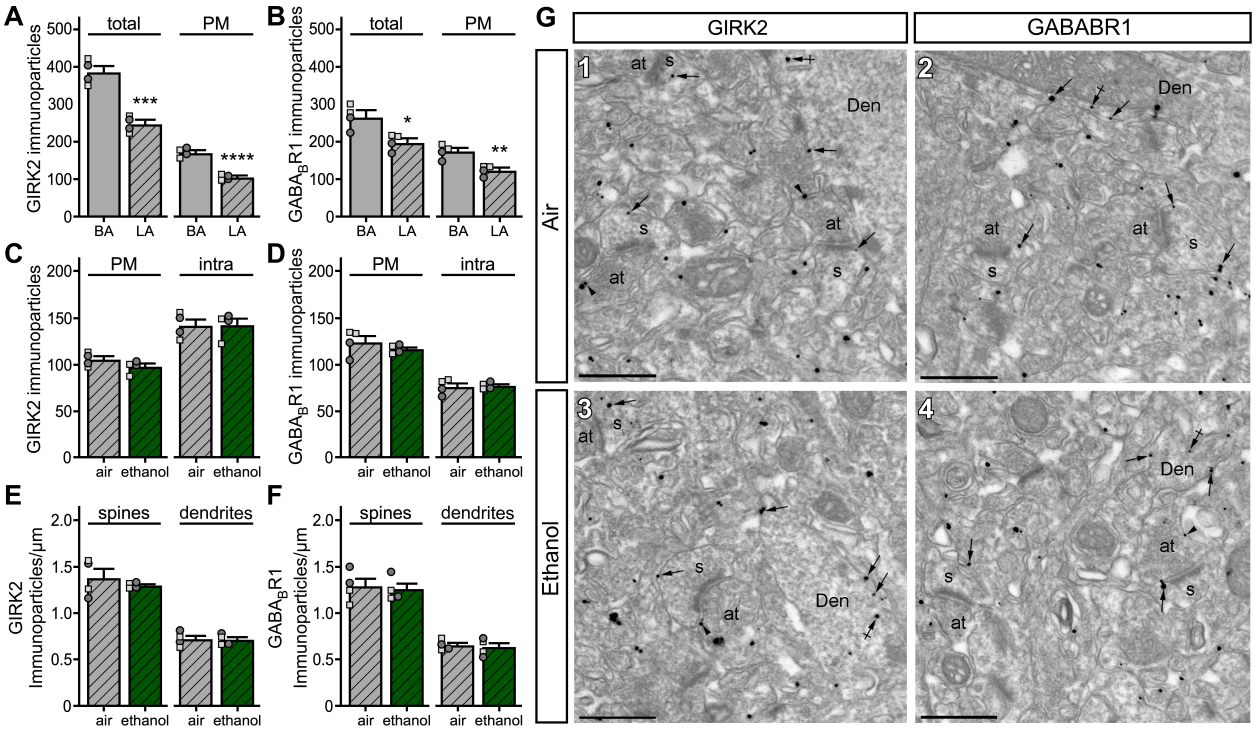

Figure S1. Ethanol exposure does not affect the subcellular localization of GIRK2 and GABA$_B$R1 in LA principal neurons

A. Distribution of total GIRK2 immunoparticles (t_6=7.140, ***P=0.0004; N=4/group; unpaired Student's t-test) and at the plasma membrane (t_6=9.226, ****P<0.0001; N=4/group; unpaired Student's t-test) in BA and LA principal neurons from air-exposed mice. The BA data presented in this graph is the same as in **Fig. 5A** (PM/Air) to aid with the comparison. The LA data (PM) is also used in **Fig. S1C** (PM/Air) to aid with the comparison; note the scale difference. Small squares and circles represent individual data points from male and female subjects, respectively.

B. Distribution of total GABA$_B$R1 immunoparticles (t_6=3.478, *P=0.0132; N=4/group; unpaired Student's t-test) and at the plasma membrane (t_6=4.262, **P=0.0053; N=4/group; unpaired Student's t-test) in BA and LA principal neurons from air-exposed mice. The BA data presented in this graph is the same as in **Fig. 5B** (PM/Air) to aid with the comparison. The LA data (PM) is also used in **Fig. S1D** (PM/Air) to aid with the comparison; note the scale difference.

C. Distribution of GIRK2 immunoparticles at the plasma membrane (t_6=1.528, P=0.1774; N=4/group; unpaired Student's t-test) and intracellular sites (t_6=0.077, P=0.9411; N=4/group; unpaired Student's t-test) in LA principal neurons from air- and ethanol-exposed mice.

D. Distribution of GABA$_B$R1 immunoparticles at the plasma membrane of spines a (t_6=1.020, P=0.3472; N=4/group; unpaired Student's t-test) and intracellular sites (t_6=0.2218, P=0.8319; N=4/group; unpaired Student's t-test) in LA principal neurons from air- and ethanol-exposed mice.

E. Plasma membrane-associated immunogold particle density for GIRK2 in spines (t_6=0.8063, P=0.4766; N=4/group; unpaired Student's t-test with Welch's correction) and dendrites (t_6=0.1241, P=0.9053; N=4/group; unpaired Student's t-test) from LA principal neurons from air- and ethanol-exposed mice.

F. Plasma membrane-associated immunogold particle density for $GABA_BR1$ in spines (t_6=0.290, P=0.7816; N=4/group; unpaired Student's t-test) and dendrites (t_6=0.400, P=0.7029; N=4/group; unpaired Student's t-test) from LA principal neurons from air- and ethanol-exposed mice.

G. Electron micrographs showing immunoparticles for GIRK2 (panels 1&2) and $GABA_BR1$ (panels 5&6) in the LA of air-exposed mice, and for GIRK2 (panels 3&4) and $GABA_BR1$ (panels 7&8) in ethanol-exposed mice. In sections from air-exposed mice, most immunoparticles for GIRK2 and $GABA_BR1$ were located along the extrasynaptic plasma membrane (arrows) of dendritic shafts (Den) and spines (s) of LA principal neurons. GIRK2 and $GABA_BR1$ immunoparticles were also detected at intracellular sites (crossed arrows). In ethanol-exposed mice, immunoparticles for GIRK2 and $GABA_BR1$ were mostly located at intracellular sites (crossed arrows), and less frequently along the extrasynaptic plasma membrane (arrows) of dendritic shafts (Den) and spines (s) of LA principal neurons. at, axon terminal. Scale bars: 500 nm.

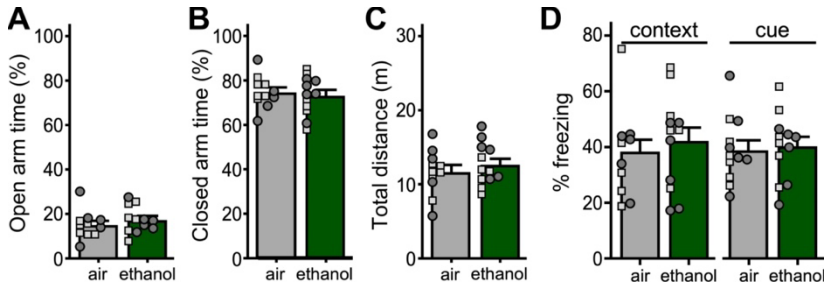

Figure S2. CIE/4 treatment in C57BL/6J mice does not impact performance in elevated plus maze or fear conditioning tests

A,B. Percentage of time spent in open (t_{21}=0.914, P=0.371; N=11-12 mice/group; Student's t-test) and closed (t_{21}=0.482, P=0.635; unpaired Student's t-test) arms of the EPM by C57BL/6J mice, measured 3 d after completing CIE/4 vapor exposure protocol. Small squares and circles represent individual data points from male and female subjects, respectively.

C. Total distance traveled during the EPM test (t_{21}=0.839, P=0.411; N=11-12/group; unpaired Student's t-test).

D. Percentage of time spent freezing during context (t_{22}=0.255, P=0.801; N=12 mice/group; unpaired Student's t-test) and cue (t_{22}=0.578, P=0.569; N=12 mice/group; unpaired Student's t-test) recall tests by air- or ethanol vapor-treated C57BL/6J mice, conducted 1 and 2 d, respectively, after fear conditioning.

SUPPLEMENTAL REFERENCES

1. Yizhar O, Fenno LE, Prigge M, Schneider F, Davidson TJ, O'Shea DJ, et al. (2011): Neocortical excitation/inhibition balance in information processing and social dysfunction. *Nature* 477:171-178.
2. Lein ES, Hawrylycz MJ, Ao N, Ayres M, Bensinger A, Bernard A, et al. (2007): Genome-wide atlas of gene expression in the adult mouse brain. *Nature* 445:168-176.
3. Farook JM, Krazem A, Lewis B, Morrell DJ, Littleton JM, Barron S (2008): Acamprosate attenuates the handling induced convulsions during alcohol withdrawal in Swiss Webster mice. *Physiol Behav* 95:267-270.
4. Sidhu H, Kreifeldt M, Contet C (2018): Affective Disturbances During Withdrawal from Chronic Intermittent Ethanol Inhalation in C57BL/6J and DBA/2J Male Mice. *Alcohol Clin Exp Re*s 42:1281-1290.
5. Vo BN, Marron Fernandez de Velasco E, Rose TR, Oberle H, Luo H, Hopkins CR, et al. (2021): Bidirectional influence of limbic GIRK channel activation on innate avoidance behavior. *J Neurosci* 41:5809-5821.
6. Tipps ME, Raybuck JD, Buck KJ, Lattal KM (2015): Acute ethanol withdrawal impairs contextual learning and enhances cued learning. *Alcohol Clin Exp Res* 39:282-290.
7. Lujan R, Nusser Z, Roberts JD, Shigemoto R, Somogyi P (1996): Perisynaptic location of metabotropic glutamate receptors mGluR1 and mGluR5 on dendrites and dendritic spines in the rat hippocampus. *Eur J Neurosci* 8:1488-1500.
8. Aguado C, Colon J, Ciruela F, Schlaudraff F, Cabanero MJ, Perry C, et al. (2008): Cell type-specific subunit composition of G protein-gated potassium channels in the cerebellum. *J Neurochem* 105:497-511.